microRNA-34a regulates neurite outgrowth, spinal morphology, and function

Massimiliano Agostini[a,1], Paola Tucci[a,b,1,2], Joern R. Steinert[a], Ruby Shalom-Feuerstein[c,d], Matthieu Rouleau[c,d], Daniel Aberdam[c,d], Ian D. Forsythe[a], Kenneth W. Young[a], Andrea Ventura[e], Carla P. Concepcion[e], Yoon-Chi Han[e], Eleonora Candi[b], Richard A. Knight[a], Tak W. Mak[f], and Gerry Melino[a,b,3]

[a]Medical Research Council, Toxicology Unit, Leicester University, Leicester LE1 9HN, United Kingdom; [b]Biochemistry Laboratory, Istituto Dermopatico dell'Immacolata/Istituto Di Ricovero e Cura a Carattere Scientifico, University of Rome "Tor Vergata," 00133 Rome, Italy; [c]Institut National de la Santé et de la Recherche Médicale U898, University of Nice Sophia Antipolis, 06107 Nice, France; [d]INSERTECH, Rappaport Family Institute for Research in the Medical Sciences, Technion–Israel Institute of Technology, Haifa 31096, Israel; [e]Cancer Genetics and Biology Program, Memorial Sloan–Kettering Cancer Center, New York, NY 10065; and [f]Campbell Family Institute for Breast Cancer Research, Princess Margaret Hospital, Toronto, ON, Canada M5G 2C1

Edited by Michael Karin, University of California, San Diego School of Medicine, La Jolla, CA, and approved November 8, 2011 (received for review July 25, 2011)

The p53 family member TAp73 is a transcription factor that plays a key role in many biological processes, including neuronal development. In particular, we have shown that p73 drives the expression of miR-34a, but not miR-34b and c, in mouse cortical neurons. miR-34a in turn modulates the expression of synaptic targets including synaptotagmin-1 and syntaxin-1A. Here we show that this axis is retained in mouse ES cells committed to differentiate toward a neurological phenotype. Moreover, overexpression of miR-34a alters hippocampal spinal morphology, and results in electrophysiological changes consistent with a reduction in spinal function. Therefore, the TAp73/miR-34a axis has functional relevance in primary neurons. These data reinforce a role for miR-34a in neuronal development.

cell death | synaptogenesis | neuronal differentiation | hippocampus

Micro-RNAs (miRs) are one family of a number of small noncoding regulatory RNAs (1). They are initially transcribed as pri-miRs, which are processed by a nuclear RNase III enzyme to form stem-loop structured premiRs. The premiRs are transported to the cytosol, where another RNase III cleaves off double-stranded portions of the hairpin to generate a short-lived dsRNA of approximately 20 to 25 nt. This duplex becomes unwound, and one strand (forming the mature miR) becomes incorporated into miR–protein complexes. The mature miR within the miR–protein complex recognizes complementary sites in the 3′ UTR of target genes, resulting in translational inhibition or destabilization of the target mRNAs and down-regulation of the encoded protein. During development, a number of miRs show distinct expression patterns during maturation of the CNS (2). For example, microarray miR profiling of embryonic, early postnatal, and adult brain revealed differential changes in nine miRNAs, including miR-9 and -124, and the levels of both these miRs increase markedly during the transition from neuronal precursors to mature neurons. miR-124 has also been implicated in the differentiation of neuroblastoma cells induced by retinoic acid (3).

p73 is a member of the p53 family. Two distinct promoters transcribe different isoforms containing—TAp73—or lacking—ΔNp73—the aminoterminal transactivation domain (4); furthermore, extensive alternative 3′-splicing produces additional isoforms (5, 6). Trp73-KO mice have significant developmental abnormalities of the central nervous system, including congenital hydrocephalus, hippocampal dysgenesis, and defects of pheromone detection (7). Isoform-selective KOs have shown both a distinct neuronal phenotype and altered tumor susceptibility (8, 9).

p53 can regulate several miRs (10). Indeed, the miR-34 family (miR-34a–c) is a p53 target (11–13), which can mimic several p53 effects in a cell type-specific manner. miR-34a is ubiquitous with the highest expression in mouse brain, and overexpression of miR-34a in neuroblastoma cell lines modulates neuronal-specific genes (14), whereas miR-34b and c are mainly expressed in the lung (15). Less information is available on miRs regulated by p73, although recently miR-193a-5p has been shown to be a p73 target (16). In a companion paper (17), we have shown that TAp73 drives the expression of miR-34a, but not miR-34b and c, in mouse cortical neurons; miR-34a in turn modulates the expression of synaptic targets including synaptotagmin-1 and syntaxin-1A, a pathway also conserved in pathological situations such as the hippocampus of patients with Alzheimer's disease (17).

Here, we have investigated the functional effects of miR-34a in the nervous system. We demonstrate that manipulation of miR-34a expression is associated with both morphological and electrophysiological changes in ES stem cells and in mouse models, thus highlighting the importance of the TAp73/miR-34a axis in neuronal differentiation and synaptogenesis.

Results

p73$^{-/-}$ and miR-34a$^{-/-}$ Mice Display Neuronal Dysgenesis. In p73$^{-/-}$ mice, the shape of the dentate gyrus (DG) is altered and the lower blade is missing or truncated (7). We asked whether this abnormal anatomy of the DG could be caused, at least in part, by the morphology of hippocampal neurons. To investigate this, we performed Golgi staining on brain coronal sections from 18-d-old WT and p73$^{-/-}$ mice. Fig. 1*A* shows that hippocampal neurons in the DG from p73$^{-/-}$ mice show a disorganized distribution and exhibit an altered morphology. This disorganization is also evident when the hippocampus was stained with anti-Calbindin antibody for the presence of cells that do not show an apical orientation (Fig. S1*A*, white arrows). Notably, p73$^{-/-}$ hippocampal neurons have a reduced number of branches and shorter dendrites than WT hippocampal neurons. Indeed, mossy fiber (i.e., Calbindin-positive) and polysialylated neural cell adhesion molecule-positive projections in CA3 of p73$^{-/-}$ mice are reduced in length (Fig. S1 *B* and *C*). Then, we analyzed the hippocampus of miR-34a$^{-/-}$ mice (18), and we observed that the architecture of the DG in miR-34a$^{-/-}$ mice is preserved compared with WT mice (Fig. S2*A*). However,

Author contributions: M.A., E.C., R.A.K., T.W.M., and G.M. designed research; M.A., P.T., J.R.S., R.S.-F., M.R., and K.W.Y. performed research; A.V., C.P.C., Y.-C.H., and T.W.M. contributed new reagents/analytic tools; M.A., P.T., J.R.S., D.A., I.D.F., and E.C. analyzed data; and M.A., R.A.K., and G.M. wrote the paper.

The authors declare no conflict of interest.

This article is a PNAS Direct Submission.

[1]M.A. and P.T. contributed equally to this work.

[2]Present address: Department of Pharmaco-Biology, University of Calabria, 87036 Rende, Italy.

[3]To whom correspondence should be addressed. E-mail: gm89@le.ac.uk.

This article contains supporting information online at www.pnas.org/lookup/suppl/doi:10.1073/pnas.1112063108/-/DCSupplemental.

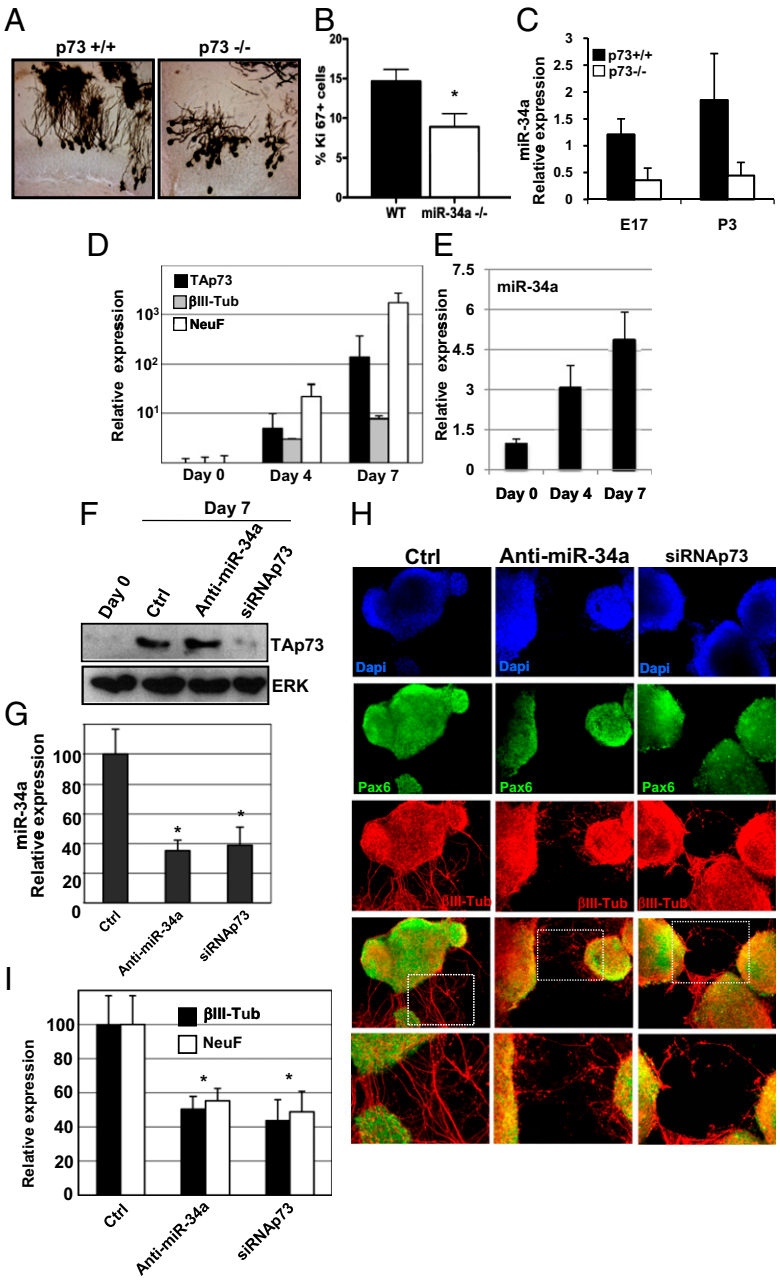

Fig. 1. The TAp73/miR-34a pathway participates in neuronal commitment of murine ES cells. (*A*) Hippocampal morphology is altered in the DG of p73$^{-/-}$ mice. Golgi staining of DG from p73$^{+/+}$ and p73$^{-/-}$ mice (age P18). Brain coronal sections were treated as described in *Methods*. A representative photomicrograph is shown. (*B*) Proliferating cells are reduced in the SGZ of miR-34a$^{-/-}$ mice. Graph shows the mean ± SD of Ki-67–positive cells. (*C*) miR-34a expression is reduced in the hippocampus of p73$^{-/-}$ mice between E17 and postnatal day 3. Hippocampus was isolated from p73$^{+/+}$ and p73$^{-/-}$ mice ($n = 3$), and levels of miR-34a were evaluated by real-time PCR (*$P < 0.05$). (*D* and *E*) Murine ES cells were cultivated on fixed feeder NIH 3T3 cells in the absence of serum, as described in *Methods*. Differentiated cells were collected at the indicated times and neural differentiation was evaluated. Real-time PCR analysis demonstrated that ES cells rapidly and efficiently differentiated into neural cells, as indicated by the induction of neural markers, such as neurofilament (NeuF) and βIII-tubulin (βIII-Tub). At the indicated times, RNA extractions were prepared for real-time PCR analysis of βIII-tubulin, neurofilament, TAp73, and miR-34a. Neural differentiation was evident at the RNA level by elevation of the putative neural markers βIII-tubulin and neurofilament. Expression of p73 and miR34a was also enhanced in parallel during differentiation. (*H*) Immunofluorescent staining was performed at day 7 of differentiation, showing typical neurite formation in control cells (Ctrl) that were also immunoreactive with Pax6 and βIII-tubulin antibodies. Merge of the same fields is shown, and higher magnification of the merged image is also shown (*Insets*). The same analysis was performed in cells transfected with anti–miR-34a or sip73 (*F* and *G*), and, in both cases, shows a reduction in Pax6 and βIII-tubulin immunoreactivity, together with reductions in neurite outgrowth. In the same experiment, changes in p73, neurofilament, and βIII-tubulin (*D*) and miR-34a (*E*) expression were examined at days 4 and 7. Change in expression of TAp73 and miR-34a at days 0 and 7 in control cells (Ctrl) and cells transfected with anti–miR-34a (*D*) or siRNAp73 (*E*) are shown along with corresponding changes in expression of βIII-tubulin and neurofilament at day 7 (*I*).

we did find a significant reduction of precursor proliferating cells (i.e., Ki-67–positive cells) in the subgranular zone of the DG in miR-34a$^{-/-}$ mice (Fig. 1*B* and Fig. S2*B*).

This hippocampal phenotype of p73$^{-/-}$, TAp73$^{-/-}$, and miR-34a$^{-/-}$ mice led us to investigate whether the TAp73/miR-34a axis could play a role in neurogenesis. First, we analyzed miR-

34a expression during hippocampal development from p73$^{-/-}$ mice between embryonic day (E) 17 and postnatal day (P) 3, when neuronal proliferation and differentiation/synapse formation is taking place (19). Fig. 1*C* shows that miR-34a expression is reduced in the hippocampus of p73$^{-/-}$ mice compared with the control mice.

Expression of TAp73 and miR-34a During Neuronal Commitment of ES Cells. Then, by using the murine ES model to explore the molecular mechanisms that underlie embryonic development of the neuroectoderm (20, 21) we addressed the role of the p73/miR-34 pathway in neurogenesis. Within 7 d of culture, large colonies with typical neural morphology were detected, which were immunoreactive for pax6 and βIII-tubulin (Fig. 1*H*), and βIII-tubulin and neurofilament mRNA levels were also increased (Fig. 1*D*). Next, we measured the expression profiles of p73 and miR-34a during neuronal ES differentiation and observed a gradual coelevation of p73 (Fig. 1*D*) and its target, miR-34a (Fig. 1*E*).

To assess the contribution of the p73/miR34 pathway to neural commitment, ES cells were transfected at day 1 of differentiation with Antago-miR34a, with siRNA that specifically targets p73 or with irrelevant oligonucleotide control sequences. As expected, siRNA against p73 reduced the expression levels of p73 protein (Fig. 1*F*). In addition, both p73-siRNA and Antago-miR34a reduced the expression levels of miR-34a, suggesting that miR-34a is also under p73 regulation during the neural differentiation of ES cells (Fig. 1*G*). Moreover, as shown in Fig. 1*H*, the inhibition of miR-34a or p73 resulted in a decrease in neurite outgrowth, as detected morphologically by immunofluorescent staining and by reduced βIII-tubulin and neurofilament mRNA levels (Fig. 1*I*). Altogether, these data suggest that p73-mediated transcription of miR-34a is required for neural embryonic neural development, particularly in the hippocampus, and for neural differentiation of ES cells.

Effect of miR-34a on Neuron Morphology. Recently, several observations have suggested that modulation of miR expression can affect the morphology of neurons (22, 23). To investigate whether miR-34a is also able to regulate the ability of neurons to develop a dendritic tree, cortical neurons at 2 d in vitro (DIV) were transfected with plasmids containing a scrambled or an miR-34a inhibitor sequence. Inhibition of miR-34a expression significantly ($P < 0.02$) increased the number of branches in cortical neurons (Fig. 2). On the contrary, ectopic expression of miR-34a resulted in a significant ($P < 0.05$) reduction of total dendritic length and branch number (Fig. 3 *A* and *B*). To evaluate the changes in complexity of the dendritic tree, we performed Sholl analysis on the same cortical neurons (24). Fig. 3*C* shows that miR-34a overexpression significantly ($P < 0.05$) reduced the complexity of the dendritic tree between 40 and 90 μm from the soma, as evaluated by number of intersections. No significant effects were observed in cortical neurons transfected with GFP or GFP plus negative control. Similar effects were obtained when experiments were carried out on hippocampal neurons (Fig. S3 *A*–*C*). Transfection of premiR-34a significantly reduced the number of branches, although the reduction in total neurite length failed to reach significance. The number of intersections was also significantly reduced between 40 and 80 μm from the cell body. To assess whether these changes were the result of changes in expression of the miR-34a target, Syt-1, we overexpressed Syt-1 (lacking the 3′UTR) in the presence of premiR-34a. Results in Fig. 3*D* and Fig. S4 show that the ectopic expression of Syt-1 partially rescues (~20%) the reduction in branch number observed in neurons overexpressing miR-34a alone. These changes in overall morphology of the dendritic tree were associated with specific changes in dendritic spine morphology, with a significant reduction in filopodia (Fig. 3*E*).

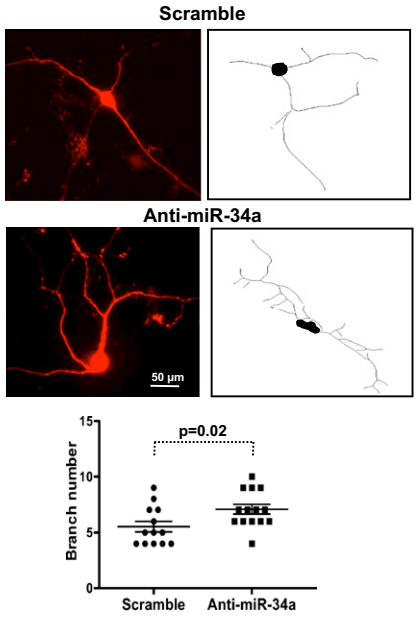

Fig. 2. miR-34a negatively affects dendritic outgrowth of cortical neurons. DIV 2 WT cortical neurons were transfected with GFP plus scramble or GFP plus anti–miR-34a (100 nM). After 72 h, neurons were fixed and mounted for confocal microscopy. A representative image is shown (*Left*). *Right*: Tracing of projections of the dendritic tree of one representative neuron. Quantification of branch number after inhibition of miR-34a was performed as described in *Methods*. In each experiment, nine to 15 cells were analyzed. Data represent mean ± SD of three different experiments (*$P = 0.02$, two-tailed Student *t* test).

Next, we investigated the effect of p73 loss on branching of cortical neurons in culture derived from WT, p73$^{-/-}$, and TAp73$^{-/-}$ mice. DIV 5 cortical neurons from both KO mice show a significant reduction in number of branches compared with WT (Fig. S5 *A* and *B*). This reduction in branching leads to a significant reduction of dendritic tree complexity, in particular between 50 and 90 μm from the cell body, as shown by Sholl analysis (Fig. S5*C*). Interestingly, the inhibition of miR-34a expression was able to partially revert the effect of TAp73 loss on branching (Fig. S5*B*).

miR-34a Affects Neuronal Function. We finally investigated whether these effects on dendritic morphology had functional consequences, in particular at the electrophysiological level. miR-34a overexpression caused a strong reduction in the number of detected events ($3.7 \pm 0.9\ s^{-1}$ vs. $8.7 \pm 1.5\ s^{-1}$; raw traces in Fig. 4 *A* and *B*). In addition, the mean miniature amplitude is reduced following miR-34a overexpression and miR-34a also induced a distinct left shift in amplitude population whereby larger events were strongly suppressed (Fig. 4*C*). The decay kinetics of miniature excitatory postsynaptic currents (mEPSCs) were also affected by miR-34a overexpression, resulting in the lack of slow-decaying events, as shown in the histogram plots in Fig. 4*D*. Conversely, when overexpressing the miR-34a inhibitor sequences, we noticed that the frequency of mEPSC recovered, and mEPSC amplitude and decay kinetics increased relative to scrambled or miR-34a expression (Fig. 4*M*). The reduction of frequency following miR-34a overexpression suggested a loss of functional synapses or release sites, whereas the decrease in mean decay kinetics (Fig. 4 *F* and *J*) pointed toward specific reductions in inhibitory signaling as those exhibit slower kinetics. To study this further, we pharmacologically isolated inhibitory and excitatory inputs. Blockade of inhibitory inputs caused a dramatic reduction of mean mEPSC frequency, amplitude, and decay kinetics (Fig. 4 *K*–*M*), thereby mimicking the effects of miR-34a overexpression. As the absence of TAp73 induced a reduction in branching, we next investigated

CELL BIOLOGY

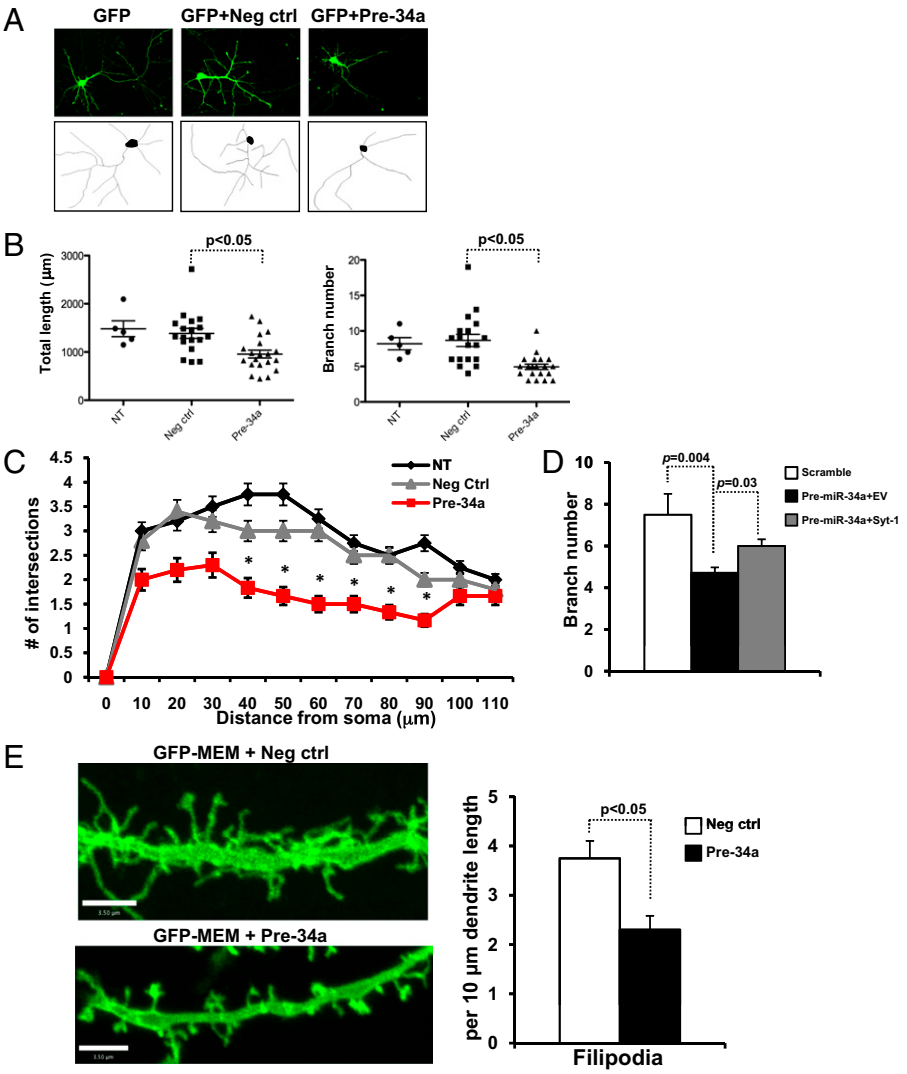

Fig. 3. miR-34a negatively affects dendritic outgrowth of cortical neurons. (*A*) DIV 2 WT cortical neurons were transfected with GFP, GFP plus scrambled control (neg ctrl), or GFP plus pre-34a (30 nM). After 72 h, neurons were fixed and mounted for confocal microscopy. Representative images are shown (*Upper*). *Lower*: Tracings of projections of the dendritic tree of one representative neuron. (*B*) Quantification of total length and branch number after ectopic expression of miR-34a was performed as described in *Methods*. (*C*) Dendritic complexity of cortical neurons transfected as in *B* was evaluated by using Sholl analysis. In each experiment, nine to 15 cells were analyzed. Data represent mean ± SD of three different experiments (**P* = 0.03, two-tailed Student *t* test). (*D*) Coexpression of Syt-1 counteracts the negative effect of miR-34a on branch number (EV, empty vector). (*E*) We overexpressed premiR-34a in hippocampal neurons, which resulted in a significant reduction in the proportion of filopodia. DIV 9 WT hippocampal neurons were transfected with GFP-MEM plus scrambled control or GFP-MEM plus Pre-34a. After 5 d, neurons were fixed and mounted for confocal microscopy; representative images are shown. The graph quantifies the number of filopodia. Data represent mean ± SD of three different experiments (****P* = 0.03, two-tailed Student *t* test).

synaptic inputs in those cultures. TAp73$^{-/-}$ data (Fig. 4 *O*–*S*) showed that synaptic signaling is also altered with a reduction in miniature excitatory junction potential amplitudes and a shift of population decay kinetics toward faster events.

Together, these data suggest that miR-34a overexpression caused changes in functional synapses as well as preferential suppression of slowly decaying inhibitory mEPSCs. Interestingly, data from TAp73$^{-/-}$ cultures indicate a dominance of smaller and faster events.

Discussion

In a companion paper, we have shown that p73 drives the expression of miR-34a, but not of the family members miR-34b and c, which have a distinct chromosomal location (17). This action is exerted through a direct binding of p73 to p53 consensus elements on the promoter of miR-34a. Consistent with this molecular relationship, miR-34a expression is modulated in parallel with that of TAp73 during in vitro differentiation of neuroblastoma cells, and cortical neurons. Retinoid-driven neuroblastoma differentiation is inhibited by silencing of p73 or miR-34a. This p73 and miR-34a link would also account for the fact that miR-34a transcript expression is significantly reduced in vivo both in the cortex and hippocampus of p73$^{-/-}$ mice and that miR-34a and TAp73 expression also increase in parallel during postnatal development of the brain and cerebellum, when synaptogenesis occurs. We have also identified two synaptic proteins as miR-34a targets; thus, overexpression or silencing of miR-34a inversely modulates expression of synaptotagmin-1 and syntaxin-1A. Finally, the TAp73/miR-34a/synaptotagmin-1 axis is conserved in brains from patients with Alzheimer's disease. In the present article, we show that the TAp73/mir-34a axis is also conserved during neuronal differentiation of ES cells. Several recent studies have demonstrated that

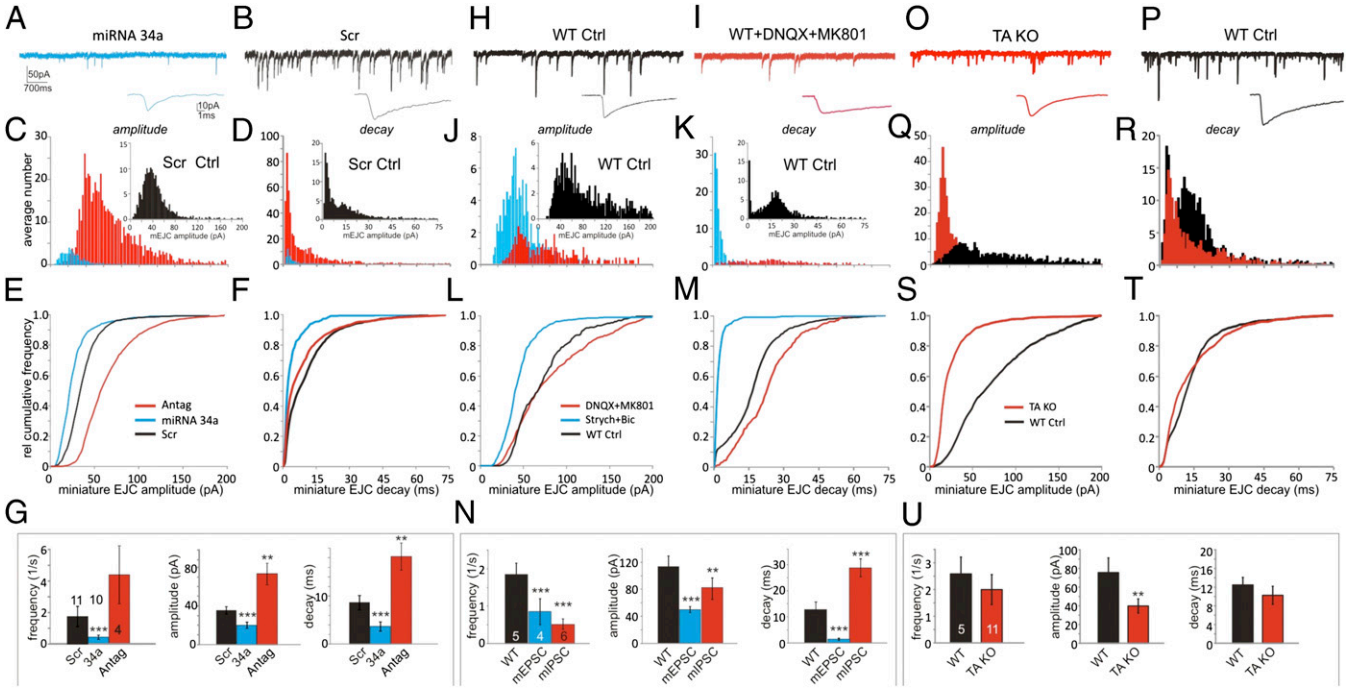

Fig. 4. Ectopic expression of miR34a produces electrophysiological changes consistent with a reduction in the number of inhibitory synapses. Electrophysiological recordings from cortical neurons were performed in the presence of 0.5 μM TTX to prevent spontaneous activity. Neurons transfected with plasmids expressing scrambled (Scr), miR-34a, or an inhibitor miR-34a sequence (Antag) were voltage-clamped and miniature events (i.e., mEPSCs) were recorded (*A–N*). mEPSCs were recorded in the presence of 0.5 μM TTX (Na^+ channel blocker) to prevent spontaneously evoked transmitter release. Cells were voltage clamped at −60 mV. miR-34a overexpression (miRNA 34a) reduced the number of mEPSCs (*A*, raw traces). Further, it also induced a leftward shift in mEPSC amplitudes and abolished slow-decaying mEPSCs (apparent as left-shifted distributions following miR-34a overexpression relative to Scr; *C–F*, blue). Conversely, inhibition of miR-34a (Antag) induced a rightward shift in amplitude and decay distributions relative to Scr (*C–F*, red). (*G*) Mean values for frequency, amplitude and decay for miR-34a, Scr, and antago-miR-34a expression (two-way ANOVA with post-hoc analysis). (*H–M*) Raw traces and amplitude and decay histograms for WT controls and pharmacologically isolated inhibitory (10 μM 6,7-dinitroquinoxaline-2,3-dione plus 50 μM MK801) and excitatory (1 μM strychnine plus 10 μM bicuculline) mEPSCs. Note that inhibition of inhibitory events following strychnine and bicuculline application mimicked the effects of miR-34a overexpression. (*N*) Mean values for frequency, amplitude, and decay following inhibition of excitatory/inhibitory inputs (two-way ANOVA with post-hoc analysis). (*O–T*) TA KO reduced the number of larger mEPSCs (*O* and *Q*) and eliminated some slow-decaying mEPSCs (*R* and *T*). (*U*) Mean values for frequency, amplitude, and decay for WT and TA KO (two-tailed Student *t* test). Data represent mean ± SEM; numbers indicated within bars (**$P < 0.01$, **$P < 0.01$, and ***$P < 0.001$).

miRs can regulate ES cell biology (25, 26). In particular, miR-134 (27), miR-124a, and miR-9 (28) are able to regulate the differentiation of ES cells toward neuronal or glial lineages. Our results indicate that miR-34a, regulated by TAp73, controls neuronal differentiation of mouse ES (mES) cells. Indeed, inhibition of miR-34a expression results in a reduction of neurite outgrowth and connectivity in neurons derived from mES cells. These data reinforce the role of TAp73 in neuronal development, with a specific emphasis on the involvement of miR-34a. However, does miR-34a have a functional impact on neuronal development?

Like p53 (29), TAp73 induces the expression of miR-34a by acting on the p53-like binding sequences on the promoter of miR-34a, although in completely distinct contexts. Therefore, miRs can be involved in distinct pathways depending on the stimuli and the cellular context. Here we show that miR-34a, in vivo and in vitro, is involved at times when synaptogenesis is taking place. Our data show that the complexity of the dendritic tree of cortical neurons, in vitro, is affected by miR-34a, possibly resulting, at least in part, from altered expression of Syt-1 and Stx-1A. Indeed, Syt-1 ectopic expression was partially able to rescue the effect of miR-34a overexpression on branch number. In addition, modulation of postsynaptic miR-34a levels affects synaptic function. Indeed, cortical neurons overexpressing miR-34a have fewer miniature events, which are a direct readout of the number of functional synapses. Additionally, the reduction of inhibitory inputs could account for the presence of fewer slowly decaying mEPSCs, leaving predominantly the fast excitatory mEPSCs, suggesting that miR-34a expression preferentially disrupts inhibitory inputs. On the contrary, the absence of TAp73 signaling in pre- and postsynaptic neurons led to altered network activities, different from the purely postsynaptic miR-34a signaling mechanisms, and this requires further investigation.

Together with those from the companion paper (17), these data therefore provide a mechanism, involving miR-34a and its synaptic protein targets, in neuronal differentiation and synaptogenesis.

Methods

Mice. The $p73^{-/-}$ and $TAp73^{-/-}$ mice were generated as previously described (7, 8). $miR\text{-}34a^{-/-}$ mice were generated in the laboratory of A.V. by homologous recombination in V6.5 ES cells. The miR-34a sequence was flanked by loxP sites. After germline transmission, the miR-34a sequence was excised by crossing with Actin-Cre mice. Complete loss of miR-34a expression was verified by qPCR and Northern blotting (A.V., C.P.C., Y.-C.H.). Mice were bred and subjected to listed procedures under the Project License released from the Home Office (United Kingdom).

Cell Culture and Transfection. Primary cortical neurons cultures were prepared from E17.5 embryos of mouse. Details are provided in *SI Methods*.

RNA Extraction and Real-Time PCR. Total RNA from cells or tissue was isolated using TRIzol (Invitrogen) according to the manufacturer's instructions. Details are provided in *SI Methods*.

Western Blot. Proteins were extracted with RIPA buffer containing mixture inhibitors (Roche) and separated on SDS-polyacrylamide gel. Details are provided in *SI Methods*.

Morphological and Electrophysiological Analysis. Neurons were transfected as indicated by using Lipofectamine 2000 at different times and analyzed 72 h or 96 h later. Details are provided in *SI Methods*. Details on Golgi staining, mES cell model and transfection, and immunofluorescence are also provided in *SI Methods*.

Statistical Analysis. All results are expressed as means ± SD (SEM for electrophysiological analysis). A P value < 0.05 was considered significant.

ACKNOWLEDGMENTS. This work has been supported by the Medical Research Council, United Kingdom; Odysseus and VIB, Belgium; grants from, "Alleanza contro il Cancro" (ACC12), MIUR/PRIN (20078P7T3K_001)/FIRB (RBIP06LCA9_0023, RBIP06LCA9_0C), AIRC (2008-2010_33-08) (#5471) (2011-IG11955), AIRC 5xmille (#9979), Italian Human ProteomeNet RBRN07BMCT, MIUR/PRIN 2008MRLSNZ_004, and Telethon Grant GGPO9133 (to G.M.). Research described in this article was also supported in part by Min. Salute (Ricerca oncologica 26/07) and IDI-IRCCS (RF06 c.73, RF07 c.57, RF08 c.15, RF07 c.57) to G.M. and E.C. Work was supported by Ministry of Education and Science of the Russian Federation (11.G34.31.0069).

1. Stefani G, Slack F-J (2008) Small non-coding RNAs in animal development. *Nat Rev Mol Cell Biol* 9:219–230.
2. Kosik K-S (2006) The neuronal microRNA system. *Nat Rev Neurosci* 7:911–920.
3. Makeyev E-V, Zhang J, Carrasco M-A, Maniatis T (2007) The MicroRNA miR-124 promotes neuronal differentiation by triggering brain-specific alternative pre-mRNA splicing. *Mol Cell* 27:435–448.
4. Kaghad M, et al. (1997) Monoallelically expressed gene related to p53 at 1p36, a region frequently deleted in neuroblastoma and other human cancers. *Cell* 90:809–819.
5. De Laurenzi V, et al. (1998) Two new p73 splice variants, gamma and delta, with different transcriptional activity. *J Exp Med* 188:1763–1768.
6. De Laurenzi VD, et al. (1999) Additional complexity in p73: Induction by mitogens in lymphoid cells and identification of two new splicing variants epsilon and zeta. *Cell Death Differ* 6:389–390.
7. Yang A, et al. (2000) p73-deficient mice have neurological, pheromonal and inflammatory defects but lack spontaneous tumours. *Nature* 404:99–103.
8. Tomasini R, et al. (2008) TAp73 knockout shows genomic instability with infertility and tumor suppressor functions. *Genes Dev* 22:2677–2691.
9. Wilhelm M-T, et al. (2010) Isoform-specific p73 knockout mice reveal a novel role for delta Np73 in the DNA damage response pathway. *Genes Dev* 24:549–560.
10. Shin S, et al. (2009) MicroRNAs that respond to histone deacetylase inhibitor SAHA and p53 in HCT116 human colon carcinoma cells. *Int J Oncol* 35:1343–1352.
11. He L, et al. (2007) A microRNA component of the p53 tumour suppressor network. *Nature* 447:1130–1134.
12. Chang T-C, et al. (2007) Transactivation of miR-34a by p53 broadly influences gene expression and promotes apoptosis. *Mol Cell* 26:745–752.
13. Raver-Shapira N, et al. (2007) Transcriptional activation of miR-34a contributes to p53-mediated apoptosis. *Mol Cell* 26:731–743.
14. Wei J-S, et al. (2008) The MYCN oncogene is a direct target of miR-34a. *Oncogene* 27: 5204–5213.
15. Bommer G-T, et al. (2007) p53-mediated activation of miRNA34 candidate tumor-suppressor genes. *Curr Biol* 17:1298–1307.
16. Ory B, et al. (2011) A microRNA-dependent program controls p53-independent survival and chemosensitivity in human and murine squamous cell carcinoma. *J Clin Invest* 121:809–820.
17. Agostini M, et al. (2011) Neuronal differentiation by TAp73 is mediated by miR-34a regulation of synaptic protein targets. *Proc Natl Acad Sci USA*.
18. Choi YJ, et al. (2011) miR-34 miRNAs provide a barrier for somatic cell reprogramming. *Nat Cell Biol* 13:1353–1360.
19. Mody M, et al. (2001) Genome-wide gene expression profiles of the developing mouse hippocampus. *Proc Natl Acad Sci USA* 98:8862–8867.
20. Gambaro K, Aberdam E, Virolle T, Aberdam D, Rouleau M (2006) BMP-4 induces a Smad-dependent apoptotic cell death of mouse embryonic stem cell-derived neural precursors. *Cell Death Differ* 13:1075–1087.
21. Rostagno P, et al. (2010) Embryonic stem cells as an ectodermal cellular model of human p63-related dysplasia syndromes. *Biochem Biophys Res Commun* 395:131–135.
22. Vo N, et al. (2005) A cAMP-response element binding protein-induced microRNA regulates neuronal morphogenesis. *Proc Natl Acad Sci USA* 102:16426–16431.
23. Fiore R, et al. (2009) Mef2-mediated transcription of the miR379-410 cluster regulates activity-dependent dendritogenesis by fine-tuning Pumilio2 protein levels. *EMBO J* 28:697–710.
24. Sholl D-A (1953) Dendritic organization in the neurons of the visual and motor cortices of the cat. *J Anat* 87:387–406.
25. Wang Y, Keys DN, Au-Young JK, Chen C (2009) MicroRNAs in embryonic stem cells. *J Cell Physiol* 218:251–255.
26. Tay Y, Zhang J, Thomson AM, Lim B, Rigoutsos I (2008) MicroRNAs to Nanog, Oct4 and Sox2 coding regions modulate embryonic stem cell differentiation. *Nature* 455: 1124–1128.
27. Tay YM, et al. (2008) MicroRNA-134 modulates the differentiation of mouse embryonic stem cells, where it causes post-transcriptional attenuation of Nanog and LRH1. *Stem Cells* 26:17–29.
28. Krichevsky AM, Sonntag KC, Isacson O, Kosik KS (2006) Specific microRNAs modulate embryonic stem cell-derived neurogenesis. *Stem Cells* 24:857–864.
29. Hermeking H (2010) The miR-34 family in cancer and apoptosis. *Cell Death Differ* 17: 193–199.